Article citation info:
Dusza M. Passenger vehicle suspension parameters influence on vehicle – track model solutions. Rail Vehicles/Pojazdy Szynowe. 2022; (3-4):3-14. https://doi.org/10.53502/RAIL-156467

Rail Vehicles/Pojazdy Szynowe

www.railvehicles.eu

# Passenger vehicle suspension parameters influence on vehicle – track model solutions

Mirosław **Dusza** [a, *]

[a] *Faculty of Transport, Warsaw University of Technology, Poland*

ARTICLE INFO

Received: 23 September 2022
Revised: 10 October 2022
Accepted: 11 October 2022
Available online: 19 October 2022

KEYWORDS

vehicle-track model
critical velocity
stability of motion
self-excited vibrations
damping of vibrations

*The simulation tests results of the rail vehicle – track system model are presented in this article. The purpose of the research was to determine the influence of chosen vehicle suspension element parameters on stability and safety of motion. Simulation model of 4-axle passengers coach was created with use the VI-Rail software. Damping component of the second stage elastic-damping element in the longitudinal direction was selected. For two values of the damping parameter applied, such a few system parameters were determined: critical velocity, values of solutions in a wide velocity range, lateral wheelset-track forces and values of safety factor against derailment. The vehicle motion was simulated along a straight track and curved track with a radius of R = 3000, 4000 and 6000 m. Comparison of vehicle model features for particular damping component values were done. The results are presented in the form of diagrams illustrating changes in the tested system parameters as a function of vehicle velocity.*



## 1. Introduction

The activity related to rail vehicle motion stability analysis have been the subject of extensive research since the introduction of motor drives [10]. The strive for increase velocity and safety of vehicle motion requires detailed analysis of many factors of the rail vehicle-track system which determining these aspirations. The research presented in the article falls under this topic and is a continuation of the authors team work [3, 4, 18–20].

A modern conventional rail vehicle has a so-called rigid wheelsets (two wheels rigidly mounted on a common axle) and 'conical' wheel profiles [5, 7]. For many years, a commonly known phenomenon associated with the motion of such a vehicle on the track is the generation of self-excited vibrations in the wheelset-track system [6, 7, 9, 10, 12–15]. In addition to the main motion (along the track), the wheelsets then make lateral displacements ($y_{lw}$) and rotational movements around the vertical axis (z). For each vehicle structure (construction), there is a range of motion velocity in which the self-excited vibrations initiated, e.g. by track irregularity are effectively damped in the system (decrease along distance). There is also a (critical) velocity characteristic of a given vehicle structure. Reaching or exceeding this value, means a significant (sadden) increase in lateral displacements of the wheelsets [9, 14, 15]. For most designs, this does not mean that the vehicle is derailed. In any case, however, the vehicle motion in conditions of coexistence of self-excited vibrations is unacceptable. Hence the desire of vehicle designers to increase the critical velocity value ($v_n$) and to ensure sufficient damping of all vibrations initiated in the vehicle-track system (by e.g.: track irregularities, cross or transition curve negotiation).

The team of authors [3, 18–20] performed extensive simulation studies of the impact of various parameters of the rail vehicle-track system model on the nature and value of solutions, with particular emphasis on determining the critical motion velocity and solutions in the overcritical velocity range. The obtained results can be equated with the dynamics of modeled (real) vehicles. A significant scope of research concerned, determining the impact of individual elements of the vehicle suspension system on the stability of model solutions. The authors of [20] noted that the

* Corresponding author: miroslaw.dusza@pw.edu.pl (M. Dusza)

elements constituting the second stage of suspension have a particularly significant impact on the value of critical velocity ($v_n$) and the value of solutions in the overcritical velocity range. Test results showing the influence of elements representing longitudinal stiffness on the second stage of suspension ($k_{2x}$) are presented in [20] (some example in Fig. 1).

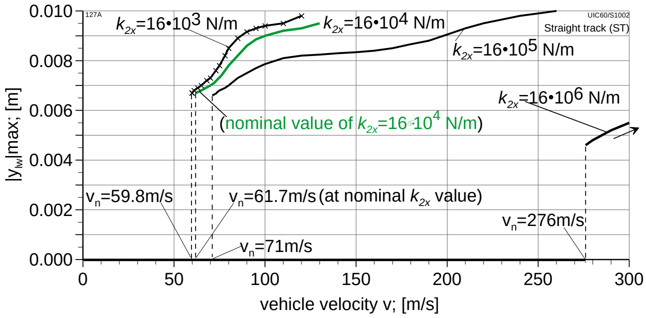


Fig. 1. The $k_{2x}$ influence on the 1-st wheelset lateral displacements in straight track [20]

It has been noticed that changes in this parameter in some range lead to a rapid increase in the critical velocity value ($v_n$) and limit the model's solutions (wheelset lateral displacements) in the overcritical velocity range. In real systems, this parameter is increased by installing additional elements between the bogie frame and the vehicle body to increase stiffness and longitudinal damping (so-called anti-yaw dampers) [2, 6].

The research presented in this article supplements the research initiated in [20]. Changes of the longitudinal damping at the second stage of suspension impact on the dynamic properties of the modeled vehicle was checked. Additional elastic-damping elements connecting the bogie frames with the car body in the longitudinal direction (along the x axis representing anti-yaw dampers) were introduced into the model. The obtained results are compared with the results of tests on a model not equipped with anti-yaw dampers (a-y dampers).

## 2. Method and range of research

### 2.1. The aim and range of research

The purpose of this research is to check the impact of the suspension second stage change in longitudinal damping on the values and character of model solutions, assuming a constant value of longitudinal stiffness (and other system parameters). Tests were carried out on a 4-axle passenger coach model moving along a straight track and in curved track with a radius of R = 3000, 4000 and 6000 m. The coach model had (additional) four elastic-damping elements connecting the bogie frames to the car body (on the left and right side of each bogie) commonly called "anti-yaw dampers". The properties of the modeled coach were examined for two types of characteristics of these elements: degressive and linear one (Fig. 3). Motion simulations were carried out in the velocity range from 10 m/s to the maximum value at which the solutions were still stable. A few parameters for the first wheelset of the coach were read from each simulation results: maximum lateral displacements $y_{lw}$ max, maximum values of lateral forces in wheelset-track contact Y and safety factor against derailment Y/Q. The obtained results were compared with the results for the vehicle model not equipped with additional elements (anti-yaw dampers).

### 2.2. The model and method of research

The model was created with the VI-Rail engineering software. This is a discrete model of a type 127A passenger coach (see Fig. 2). Bogie models are based on a 25AN construction. The complete coach model is composed of 15 rigid bodies: coach body, two bogie frames, four wheelsets and eight axle-boxes. Rigid bodies are connected with elastic-dumping elements having linear and bi-linear characteristics.

The coach model is complemented by vertically and laterally flexible track model. Track parameters corresponding to European ballasted track of 1435 mm gauge were adopted. Nominal profiles of S1002 wheels and UIC60 rails with the inclination 1:40 were used. The non-linear contact parameters are calculated with the ArgeCare RSGEO software. For calculating tangential wheel-rail contact forces, simplified Kalker theory implemented as the FASTSIM procedure is used [8, 11]. Motion equations are solved with use of the Gear procedure [12] (suitable especially to solve stiff ordinary differential equations typical to rail vehicle models description). The vehicle-track model has 83 degrees of freedom. A more detailed description of the model can be found in [3, 4, 20]. Parameters applied in research are collected in Appendix. The only difference applied to the model here is introduction of four stiff-dumping elements denoted $k_{2x}$ and $c_{2x}$ (in series) visible on the diagram (Fig. 2c). These elements connect bogie frame and car body and increase the second stage longitudinal stiffness and damping. The stiffness components are constant $k_{2x}$ = = 30 MN/m. But the damping components $c_{2x}$ changes according to the diagram presented in Fig. 3.

Two values of the damping component $c_{2x}$ were applied: 20 kNs/m and 200 kNs/m. They are called degressive (dd) and linear (ld) damper respectively, although for small velocity of displacements (±0.1 m/s) their diagrams are cover.

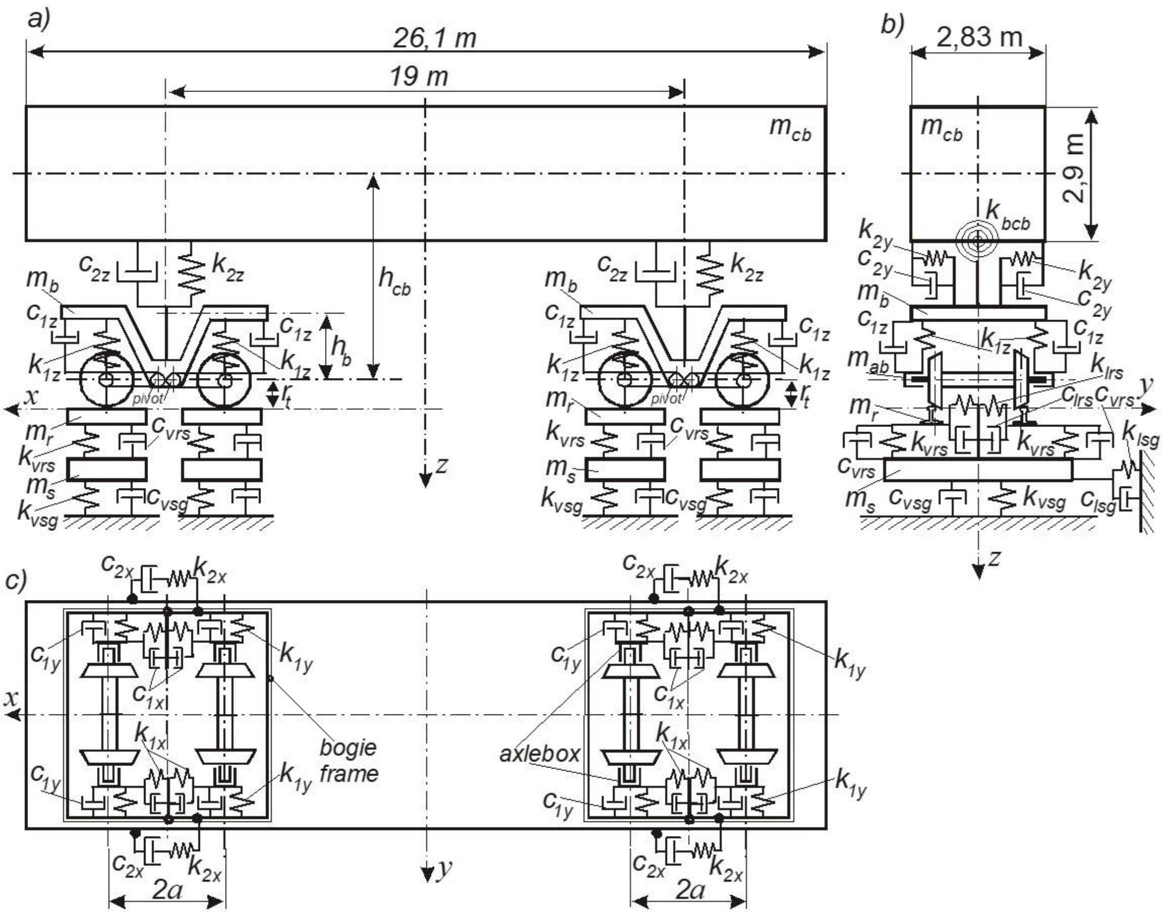


Fig. 2. Tested vehicle-track model diagram: a) side view, b) front view, c) top view

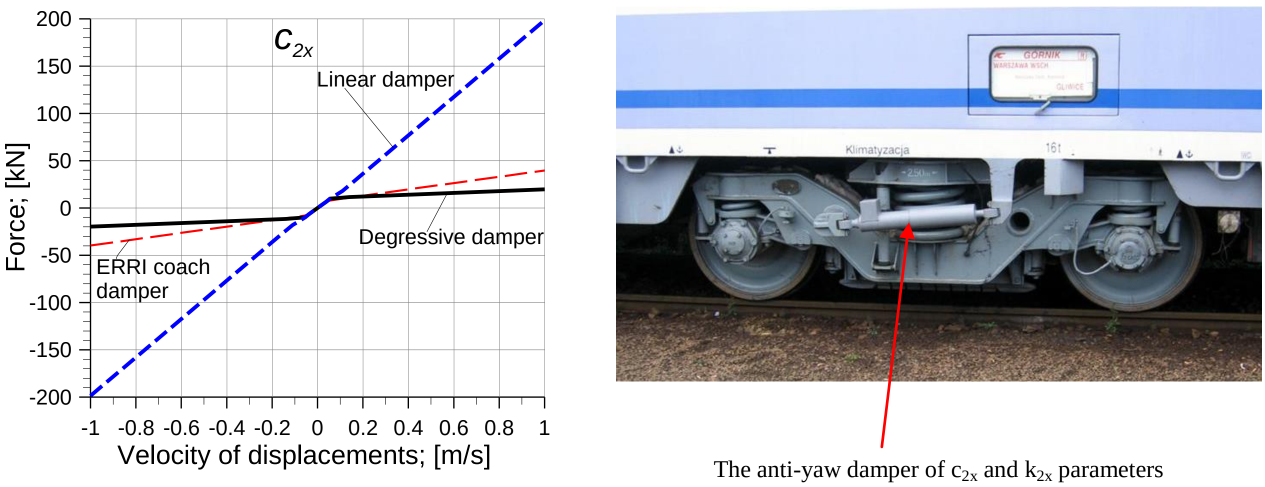


The anti-yaw damper of $c_{2x}$ and $k_{2x}$ parameters

Fig. 3. Diagram of the $c_{2x}$ component of anti-yaw damper and its location in the vehicle

The line of ERRI coach a-y damper is presented for comparison only. So, the applied $c_{2x}$ values are two times smaller (dd) and five times bigger (ld) than the ERRI standard value.

Detailed description the method of research vehicle stability can be found in publications [3, 4, 18–20]. It consists in analysing model solutions for constant vehicle velocity value. The velocity range starts from e.g. 10 m/s and ends with maximum value for which stable model solutions can be observed. The observed parameters are usually the first wheelset lateral displacements $y_{lw}$ as a function of distance or time. The „stable solution" term was adopted to describe the model solutions in which $y_{lw}$ has a constant or periodic value of the limit cycle nature. Other forms of solutions are described as unstable, although they may meet the criteria of e.g. technical stability [1]. Such criteria were also adopted in the analyses presented in this article.

Figure 4 presents examples of stable solutions typical for vehicle motion velocity lower than critical ($v < v_n$, Fig. 4a), and higher than critical ($v > v_n$, Fig. 4b).

In this example, the vehicle model motion takes place on a route consisting of a straight section (St), a transition curve (Tc) and a circular arc with a radius of R = 3000 m. The wheelset is shifted laterally during transition curve negotiation and $y_{lw} \neq 0$ in regular arc section due to track superelevation appliance. Values of the superelevation in particular curve tracks are collected in Table 1. The transition curve negotiation constitute also the way to put on initial conditions, indispensable to initiate periodic solutions in curved track if other motion parameters are fulfilled (vehicle velocity equal or bigger than $v_n$ usually, Fig. 4b).

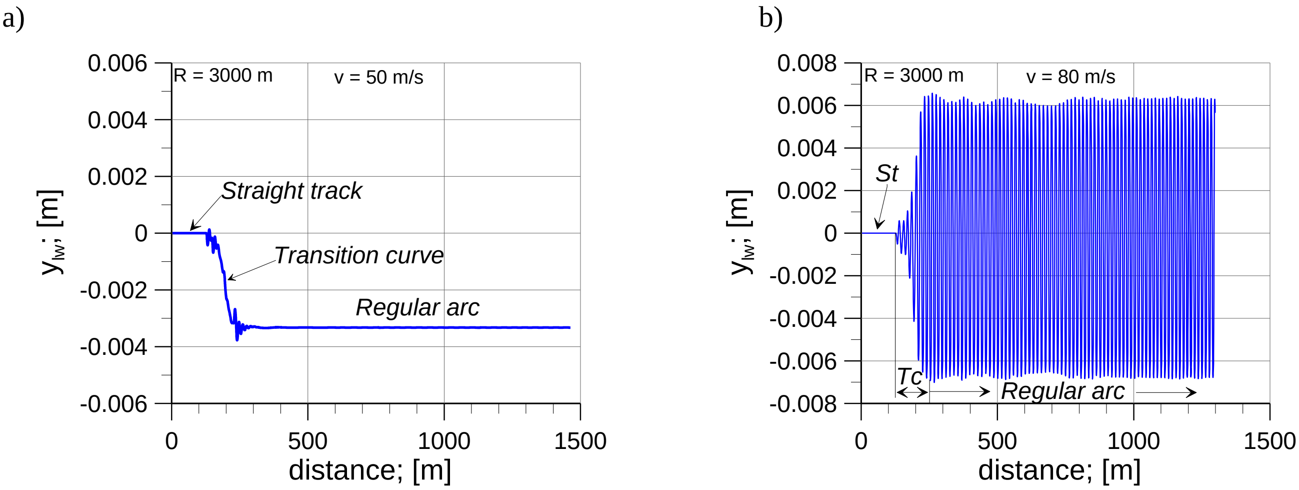


Fig. 4. The first wheelset lateral displacements $y_{lw}$ versus distance: a) stable stationary solutions (50 m/s < $v_n$), b) stable periodic solutions (limit cycle, 80 m/s > $v_n$)

Table 1. Curve radii tested and track superelevation corresponding to them

| | | | | | | |
|---|---|---|---|---|---|---|
| Curve radius R [m] | 1200 | 2000 | 3000 | 4000 | 6000 | ∞ |
| Superelevation h [m] | 0.150 | 0.130 | 0.110 | 0.077 | 0.051 | 0 |

## 3. The results

To make possible assess of the anti-yaw dampers influence on vehicle properties, so-called stability map prepared for vehicle without anti-yaw dampers is presented in Fig. 5. It present couple of diagrams – maximum of leading wheelset lateral displacements absolute value ($|y_{lw}|$max) versus vehicle velocity and peak to peak value of the $y_{lw}$ versus velocity too.

Main information enable to observe on the diagrams are as follows:

- stable stationary solutions exists on each curved track for velocity lower than 61.7 m/s,
- the smallest critical velocity (61.7 m/s) appears in straight track,
- critical velocities in curved tracks are a few m/s bigger than in straight track,
- R = 2000 m is the smallest curve radius for which periodic solutions appears,
- upper velocity limit at which stable periodic solutions exists increase according to curve radius increase,
- both observed parameters ($|y_{lw}|$max and p-t-p $y_{lw}$) increase according to curve radius increase in the over critical velocity range,
- stable periodic solutions exists for velocity increased up to about 130 m/s (in straight track and curved track of R = 6000 m). The range decrease for smaller curve radii.

Currently the range of research cover motion along straight track and curved track of curve radius R = = 3000, 4000 and 6000 m for the model equipped with the a-y dampers. Series of simulations for constant value of vehicle velocity were performed. The smallest value of apply velocity is 10m/s. The maximum velocity value applied, correspond to these values of velocity for which stable solutions exists yet (stationary or periodic one). But diagrams presented below show results up to 150 m/s, due to unrealistic velocity possible to apply for real (modelled) vehicle (150 m/s = 540 km/h).

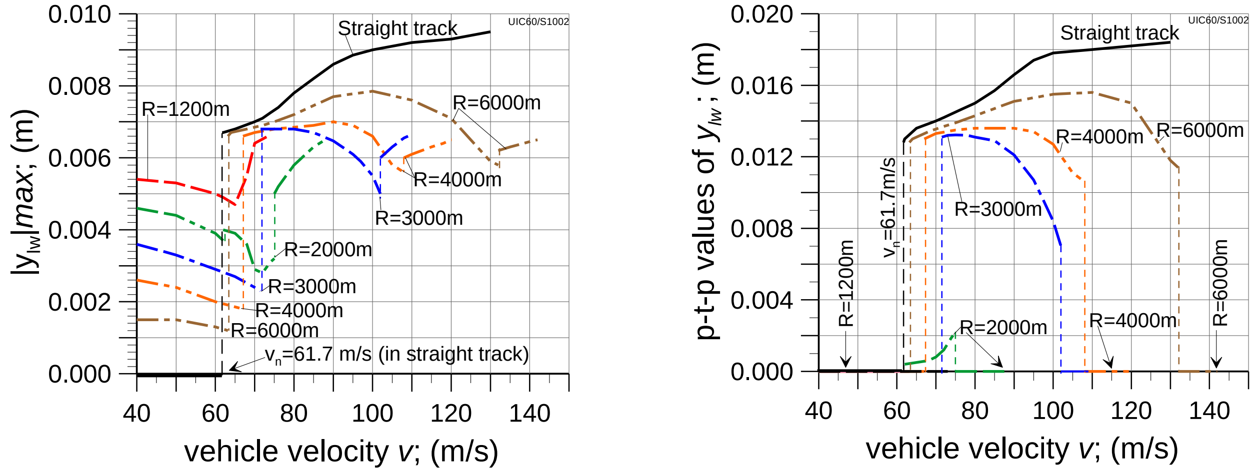


Fig. 5. Maximum of leading wheelset lateral displacements absolute value ($|y_{lw}|max$) and peak-to-peak values of $y_{lw}$ versus vehicle velocity. Model without the anti-yaw dampers

Couple of diagrams show in Fig. 6 and 7 present maximum of the leading wheelset lateral displacements absolute value versus vehicle velocity in straight track and curved track of curve radius R = = 3000, 4000 and 6000 m for degressive (dd) and linear a-y damper (ld) respectively. Stable stationary solutions ($y_{lw}$ = 0) exists in straight track for velocity lower than 107.9 m/s (dd) and 118.4 m/s (ld). Then bifurcation to stable periodic solutions appears. Diagrams present results for velocity up to 150 m/s, but stable periodic solutions exists for velocity bigger than 200 m/s in straight track. The $|y_{lw}|max$ slightly increase according to vehicle velocity increase in the over critical velocity range. So, the a-y dampers characteristic influence on $v_n$ value as well as on the $|y_{lw}|max$ at velocity $v_n$, $|y_{lw}|max \cong 0.0062$ m for (ld) a-y dampers and $|y_{lw}|max \cong 0.0072$ m for (dd) a-y dampers.

Stable stationary solutions exists in the initial velocity range in curved tracks. But wheelset does not take central position in track ($y_{lw} \neq 0$) due to superelevation appliance (Table 1). The smallest critical velocity $v_n$ = 63.8 m/s was observed in curve of R = 3000 m. The tested a-y damper characteristic does not influence on this value. Stable periodic solutions exists in the over critical velocity range up to about 90 m/s (for dd) and 102 m/s (for ld). The biggest critical velocities in curves appears for R = 4000 m, $v_n$ = 104.8 m/s (for dd) and 103.6 m/s (for ld). Stable periodic solutions exists for velocity increased up to about 115 m/s (for dd) and 116 m/s (for ld). In both curves of R = 3000 and 4000 m, there exists some velocity range of stable stationary solutions at the final segment of stable solutions existence. It is effect of centrifugal force acting on the vehicle in curve. Big velocity in curve generate large centrifugal lateral forces which „damp" the wheelset lateral displacements.

Critical velocity values $v_n$ = 75.9 m/s (for dd) and 78.4 m/s (for ld) appears for curve radius R = 6000 m. But the stable periodic solutions exists up to 80.3 m/s (for dd) and 80.2 m/s (for ld) only. Then the solutions lose their limit cycle character for velocity bigger than mentioned. The p-t-p values of $y_{lw}$ change and although they are limited and observable they can not be accepted as a stable solutions. So, the lines for R = = 6000 m presents $|y_{lw}|max$ observed on the analysed track distance for particular vehicle velocities, but the $y_{lw}$ are not periodic and not stationary as well. Some examples for velocity: 85, 100, 130 and 145 m/s are presented in Fig. 8. The solutions does not take stationary or periodic character again until the end of observable solution existence (vehicle velocity about 145.2 m/s).

The next pair of diagrams presents first wheelset – track lateral forces Y for degressive dampers (Fig. 9) and linear dampers (Fig. 10). Quite small values of the Y are observed for velocity smaller than $v_n$ for straight track and particular curves. The Y change of sign in curves at velocity about 60 m/s is an effect of superelevation appliance. Significant increase of the Y at critical velocity value achievement is observed in straight track. The Y change periodically for velocity bigger than $v_n$ according to periodic wheelset lateral displacements. So, the diagrams presents maximum value of Y ($Y_{max}$) observed for particular vehicle velocity. High value of Y may be the cause of track damage. The limited value of wheelset - track lateral force $\Sigma Y_{(2m)}$ for modelled vehicle, was assess to about 40 kN [4]. This value result from the possibility of permanent track displacement (rails and sleepers versus ballast) due to high value of lateral force acting. The way of $\Sigma Y_{(2m)}$ determination correspond to so called the Prud'homme' criterion [16].

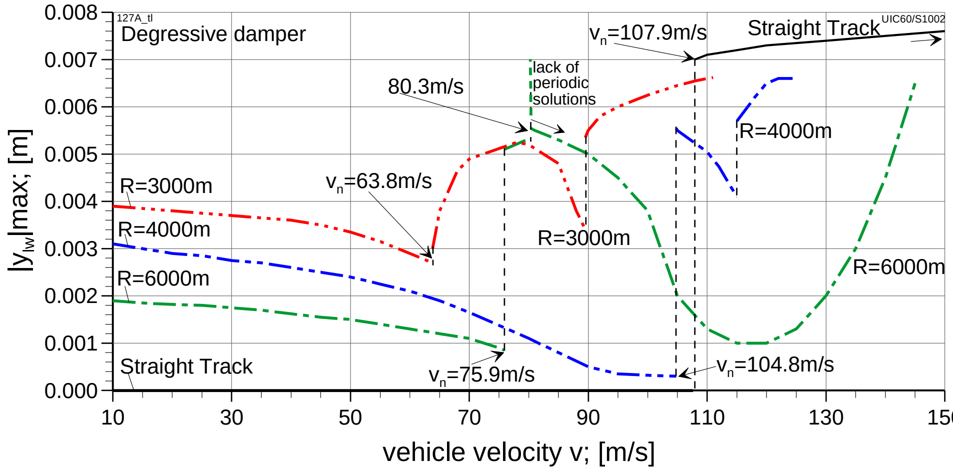


Fig. 6. Maximum of the leading wheelset lateral displacements absolute value versus vehicle velocity in straight track and curved track of curve radius R = 3000, 4000 and 6000 m. Degressive a-y dampers (dd) applied

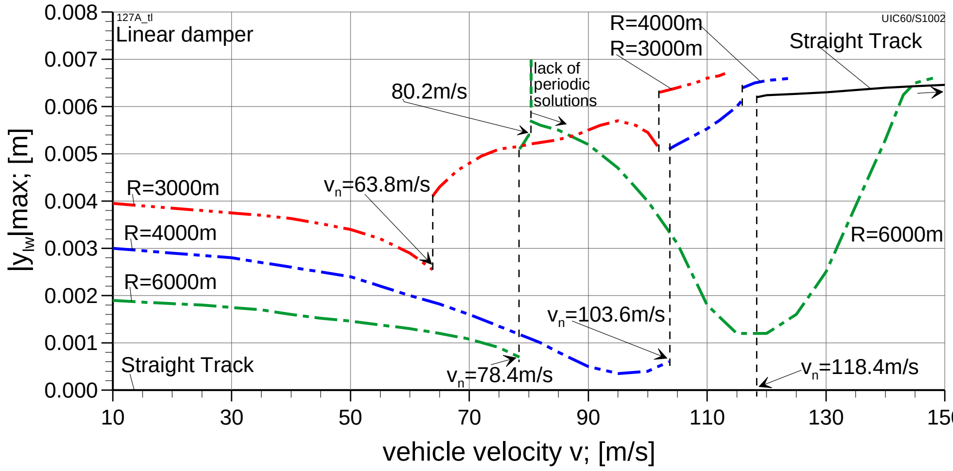


Fig. 7. Maximum of the leading wheelset lateral displacements absolute value versus vehicle velocity in straight track and curved track of curve radius R = 3000, 4000 and 6000 m. Linear a-y dampers (ld) applied

a) b)

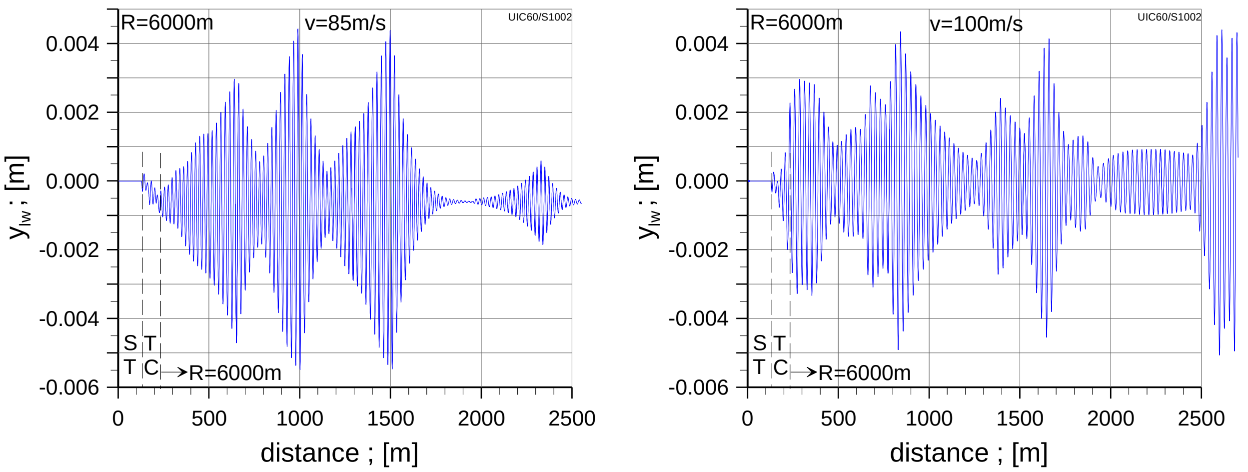


Fig. 8. The leading wheelset lateral displacements $y_{lw}$ versus distance consist of: straight track section (ST), transition curve (TC) and regular arc R = 6000 m. Vehicle velocity v: a) 85 m/s, b) 100 m/s, c) 130 and d) 145 m/s

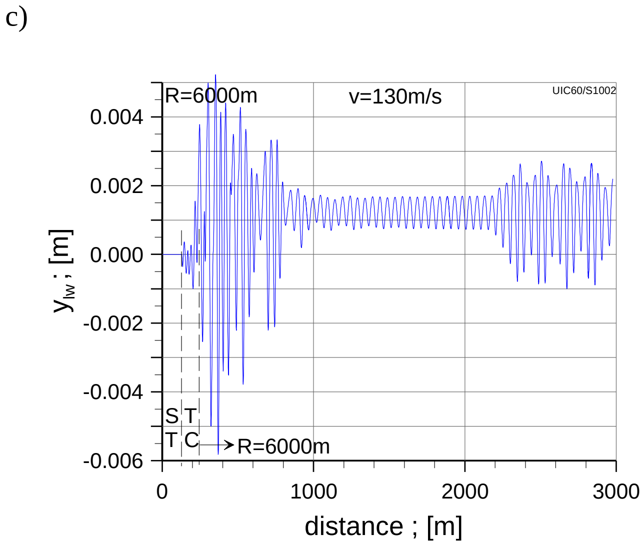


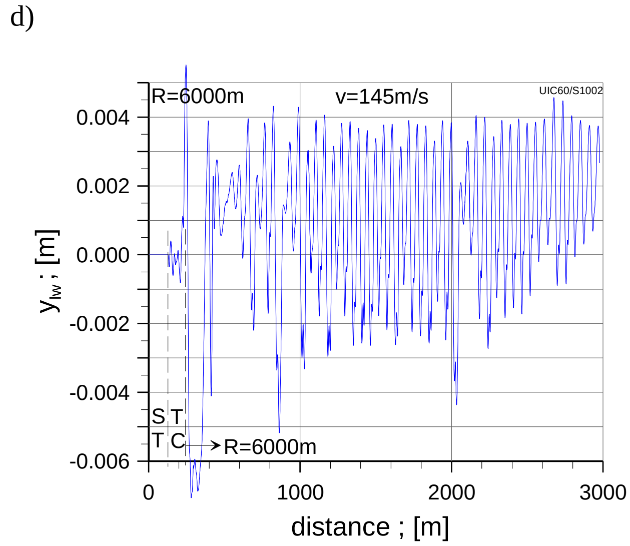


Fig. 8cd. The leading wheelset lateral displacements $y_{lw}$ versus distance consist of: straight track section (ST), transition curve (TC) and regular arc R = 6000 m. Vehicle velocity v: a) 85 m/s, b) 100 m/s, c) 130 and d) 145 m/s

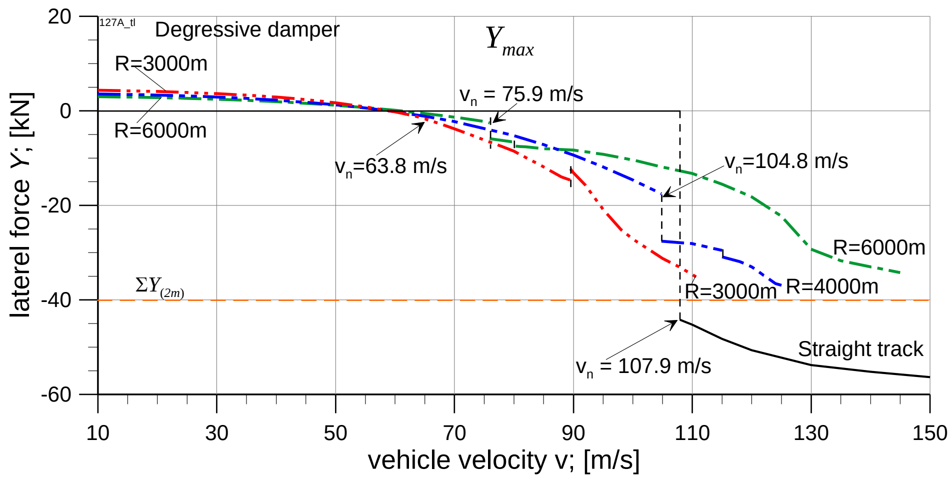


Fig. 9. The leading wheelset-track lateral forces versus vehicle velocity in straight track and curved track of curve radius R = 3000, 4000 and 6000 m. Degressive a-y dampers applied

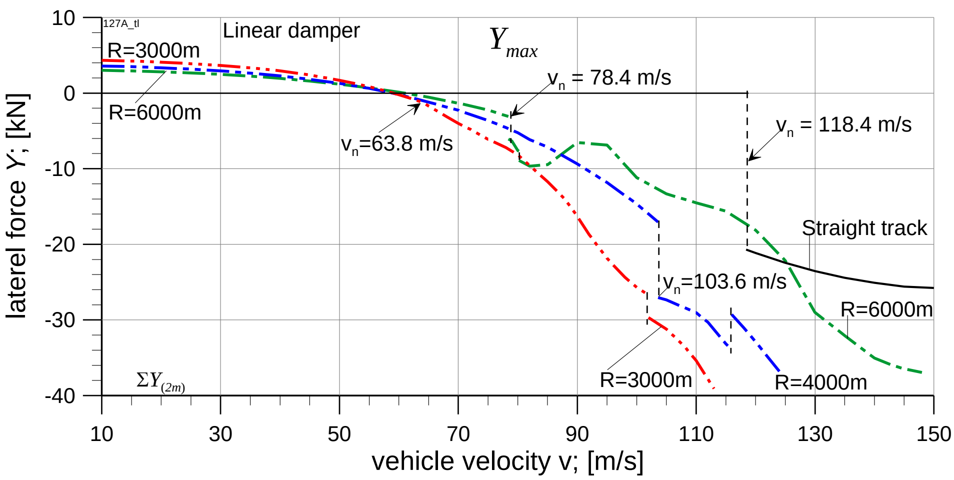


Fig. 10. The leading wheelset-track lateral forces versus vehicle velocity in straight track and curved track of curve radius R = 3000, 4000 and 6000 m. Linear a-y dampers applied

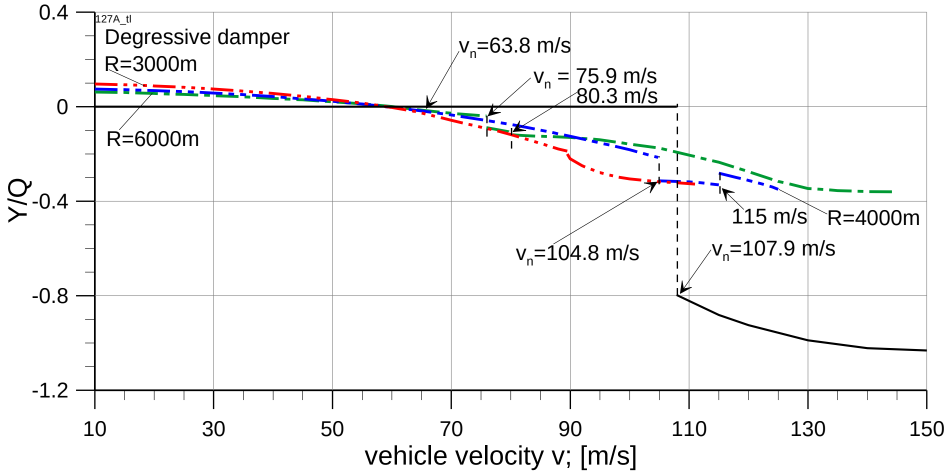


Fig. 11. Derailment ratio (Y/Q) versus vehicle velocity in straight track and curved track of curve radius R = 3000, 4000 and 6000 m. Degressive a-y dampers applied

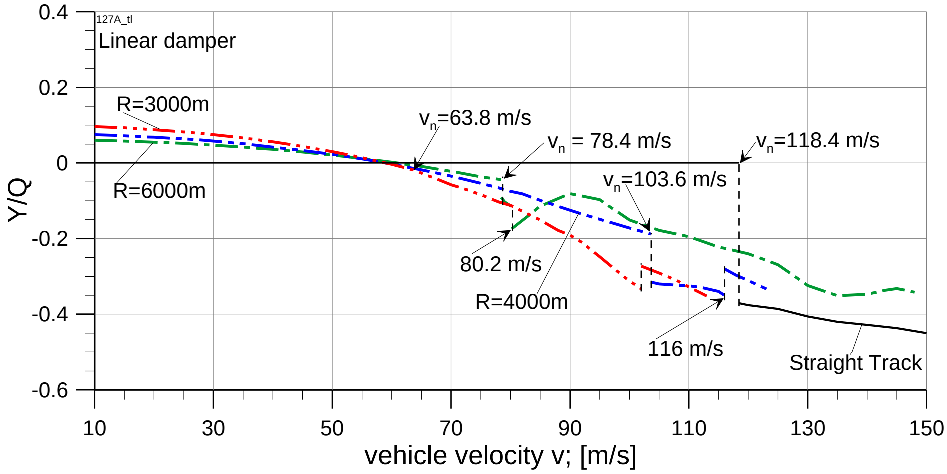


Fig. 12. Derailment ratio (Y/Q) versus vehicle velocity in straight track and curved track of curve radius R = 3000, 4000 and 6000 m. Linear a-y dampers applied

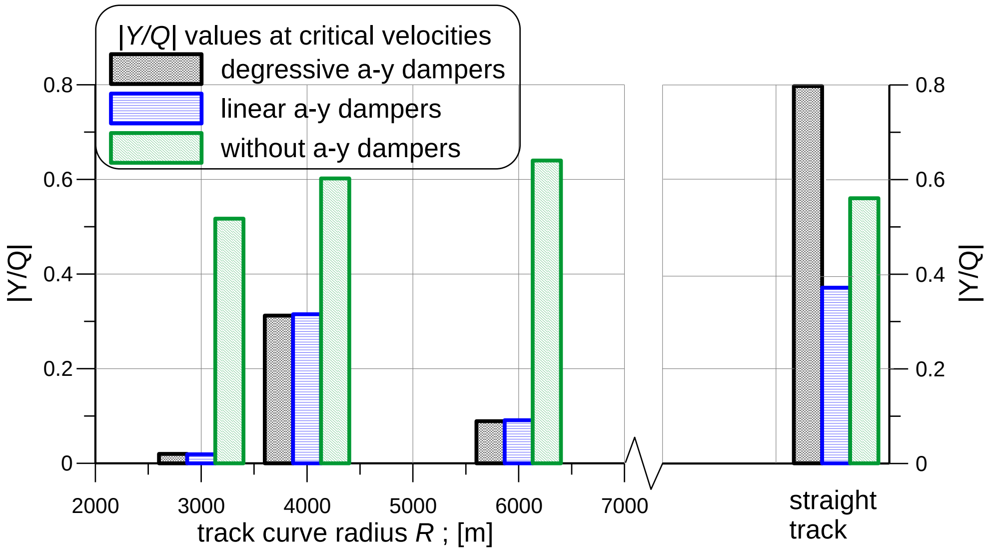


Fig. 13. Comparison of a-y dampers influence on derailment ratio (|Y/Q|) at critical velocities $v_n$ (collected in Table 2) in straight track and curved track of curve radius R = 3000, 4000 and 6000 m

So, possibility of track damage in straight section exists at critical velocity achievement for vehicle with dd a-y dampers appliance. But the limited value of lateral force $\Sigma Y_{(2m)} = 40$ kN is not excided in case of ld a-y dampers appliance (Fig. 10). Smaller (than in straight track) increases of lateral force at critical velocity in curves are observed. The lateral force increase in the over critical velocity range but does not excide the limited value 40 kN.

The quotient of lateral Y to vertical Q force of the first wheelset – track contact area is presented in the next pair of diagrams (Fig. 11 and 12). Derailment ratio - the quotient is called in short. In common opinion derailment ratio value should not excide 1.2 [5, 17]. Maximum of Y/Q values are observed in straight track for dd a-y dampers appliance. Smaller Y/Q values in curves appear. Significant influence of a-y dampers characteristic on Y/Q values in straight track is observed. But the Y/Q quotient are similar for dd and ld a-y dampers in curves. In any case the Y/Q quotient does not excide 1.2. Negative value of the Y/Q coefficient in the diagrams results from the directions of the coordinate systems adopted in the model.

Critical velocity $v_n$ is crucial parameter to presented investigations. The a-y dampers influence on $v_n$ value for particular curves is collected in Table 2. It can be noticed that the a-y dampers appliance increase critical velocity value generally. But decrease of $v_n$ is observed in case of the smallest curves of R = 3000 m. So, the a-y dampers influence on vehicle critical velocity in curves is not as unambiguous as in straight track. Comparison of the a-y dampers influence on Y/Q ratio at critical velocity $v_n$ for particular curves is presented in Fig. 13. Significant decrease of Y/Q as a result of a-y dampers appliance can be noticed. Straight track is exception here. It comes from significant differences between $v_n$ value in the model without a-y dampers (61.7 m/s) and model with the a-y dampers appliance (107.9 and 118.4 m/s). Bigger wheelset-track lateral forces are generated for bigger velocity in the overcritical velocity range.

The model stable solutions are identify to real object (modelled vehicle) possibility of motion. Velocities lower than the critical value constitute the range of normal (safe) operating velocities of the vehicle. Reaching the critical velocity (bifurcation of the model's stationary solutions to periodic solutions) is equated with the appearance of self-excited vibrations in the modelled system and provides information about approaching the maximum velocity with which the modeled vehicle can be operated. However, it does not mean a loss of motion stability. From the theoretical point of view, in the velocity range, in which there are periodic solutions (self-excited vibrations in the real system), it is possible the main vehicle motion execution. Therefore, the desirable feature of the modeled vehicle is the existence of a critical velocity and the existence of stable periodic solutions in the widest possible supercritical velocity range. Table 3 lists the velocity ranges in which there are stable periodic solutions for particular curves. As can be seen, on a straight track, the use of a-y dampers extends this range to values greater than 200 m/s. In curves, these ranges are shortened. For example, on a curve with a radius of R = 6000 m from approx. 68 m/s for a system without a-y dampers down to a few m/s for a-y dampers appliance. So, generally the a-y dampers influence on vehicle properties in curves and in straight track may be significantly different.

Table 2. The a-y dampers influence on critical velocity values

| Curve radius | Without a-y dampers | Degressive a-y dampers | Linear a-y dampers |
|---|---|---|---|
| R [m] | $v_n$ [m/s] | $v_n$ [m/s] | $v_n$ [m/s] |
| 3000 | 71.5 | 63.8 | 63.8 |
| 4000 | 67 | 104.8 | 103.6 |
| 6000 | 63.2 | 75.9 | 78.4 |
| ∞ | 61.7 | 107.9 | 118.4 |

Table 3. The a-y dampers influence on model solutions

| Velocity ranges of stable periodic solutions existence | | | |
|---|---|---|---|
| Curve radius | Without a-y dampers | Degressive a-y dampers | Linear a-y dampers |
| R [m] | v [m/s] | v [m/s] | v [m/s] |
| 3000 | 71.5–102 | 63.8–89.5 | 63.8–102 |
| 4000 | 67–108 | 104.8–115 | 103.6–116 |
| 6000 | 63.2–132 | 75.9–80.3 | 78.4–80.2 |
| ∞ | 61.7–130 | 107.9–more than 200 | 118.4–more than 200 |

## 4. Conclusions

Increase of longitudinal damping at second stage of passenger vehicle suspension has great influence on vehicle properties, especially in straight track. Increase of critical velocity is observed according to $c_{2x}$ increase. Decrease of the wheelset's lateral displacements $|y_{lw}|$max according to $c_{2x}$ increase in over critical velocity range is the second positive feature. Stable periodic solutions exists above 150 m/s of vehicle velocity for a-y dampers appliance and no mater of $c_{2x}$ characteristic. The $c_{2x}$ characteristic has great influence on wheelset – track lateral force (Y) in the over critical velocity range. Bigger $c_{2x}$ result smaller value of Y (and track damage prevention). The derailment ratio (Y/Q) depend on the $c_{2x}$ as well. Y/Q decrease according to $c_{2x}$ increase.

But in curves the $c_{2x}$ influence on vehicle properties depend on curve radius R. The critical velocity may slightly decrease for $c_{2x}$ increase (R = 3000 m). The Y and Y/Q increase at critical velocity in curves are not as big as in straight track. So, the a-y dampers appliance has not unambiguous influence on vehicle properties in curves.

The damping component $c_{2x}$ is realized by hydraulic damper in practice usually. To refer the results to practice it should be mentioned that all hydraulic dampers have some flexibility in series with the viscous damping, due to the flexibility of the hydraulic oil, damper structure, bushes and mounting brackets. The $k_{2x}$ component represent this flexibility in series with $c_{2x}$ in presented research. The adopted value of $k_{2x}$ = 30 MN/m is arbitrary. In some researchers opinion [6], the series stiffness is beneficial by reducing the transmission of unwanted high frequencies through the damper. In case of the a-y dampers the series stiffness $k_{2x}$ play key roll to control bogie kinematic motions and maintain stability. It may to sum up (partially or entirely) with the nominal value of $k_{2x}$ = = 160 kN/m at second suspension stage (see appendix) in some vehicle conditions of motion. Then, a significant increase in the longitudinal stiffness in the second suspension stage occurs. Increasing the longitudinal stiffness in the second suspension stage, due to the summation of the nominal $k_{2x}$ value and the series stiffness in the a-y damper can significantly change the model properties for the same (fixed) $c_{2x}$ characteristic. Thus, the correct selection of the $k_{2x}$ series stiffness is a separate research problem not discussed in the presented article.

To conclude the obtained results generally, positive influence of the a-y dampers on vehicle properties in straight track is observed. But unexpected vehicle features may appears in case of curved track motion.

**Acknowledgements**

This work was supported by the National Center for Research and Development (NCBiR), Poland, under the TANGO program no. – TANGO-IV-A/0027/2019-00.

## Nomenclature

$y_{lw}$ the leading wheelset lateral displacements
$v_n$ nonlinear critical velocity
Y/Q derailment ratio
R curved track radius
h track superelevation

## Bibliography

[1] Bogusz W. Technical stability (in Polish Stateczność techniczna). PWN. Warsaw 1972.
[2] Bruni S, Vinolas J, Berg M, Polach O, Stichel S. Modeling of suspension components in a rail vehicle dynamics context. Vehicle Syst Dyn. 2011;49(7): 1021-1072. https://doi.org/10.1080/00423114.2011.586430
[3] Dusza M, Zboiński K. The wheel-rail coefficient of friction influence on rail vehicle models lateral stability – bifurcation approach. Proceedings of 14th Mini Conference on Vehicle System Dynamics, Identification and Anomalies. Budapest, 10-12 November 2014: 123-134.
[4] Dusza M. Rail vehicle model possibility of safe motion analysis in the overcritical velocity range. Proceedings of the 11th International Conference on Railway Bogies and Running Gears. In: Zobory I. (Ed.), SSME/GTE, Budapest, 2020:159-168.
[5] European Standard PN-EN 14363+A1:2019-02.
[6] Evans J, Berg M. Challenges in simulation of rail vehicle dynamics. Vehicle Syst Dyn. 2009;47(8): 1023-1048. https://doi.org/10.1080/00423110903071674
[7] Iwnicki S. (ed.). Handbook of railway vehicle dynamics. CRC Press Inc. 2019. https://doi.org/10.1201/9780429469398
[8] Kalker JJ. A fast algorithm for the simplified theory of rolling contact. Vehicle Syst Dyn. 1982;(11):1-13. https://doi.org/10.1080/00423118208968684
[9] Kass-Petersen C, True H. A bifurcation analysis of nonlinear oscillations in railway vehicles. Vehicle Sys Dyn. 1984;(13):655-665. https://doi.org/10.1080/00423118308965288
[10] Knothe K, Böhm F. History of stability of railway and road vehicles. Vehicle Syst Dyn. 1999;(31):283-323. https://doi.org/10.1076/vesd.31.5.283.8362

[11] Piotrowski J. Kalker's algorithm Fastsim solves tangential contact problems with slip-dependent friction and friction anisotropy. Vehicle Syst Dyn. 2010; 48(7):869-889.
https://doi.org/10.1080/00423110903178495

[12] Shabana AA, Zaazaa KE, Sugiyama H. Railroad Vehicle Dynamics: A Computational Approach. Taylor & Francis LLC and the CRC. 2008.

[13] Sun J, Meli E, Cai W, Gao H, Chi M, Rindi A et al. A signal analysis based hunting instability detection methodology for high-speed railway vehicles. Vehicle Syst Dyn. 2021; 59(10):1461-1483.
https://doi.org/10.1080/00423114.2020.1763407

[14] True H, Jensen JC. Parameter study of hunting and chaos in railway vehicle dynamics. In: Shen Z. (Ed.) Proc. 13th IAVSD Symposium on The Dynamics of Vehicles on Roads and on Tracks. Vehicle Syst Dyn. 1994;(23):508-520.

[15] True H. On the theory of nonlinear dynamics and its applications in vehicle systems dynamics. Vehicle Syst Dyn. 1999;(31):393-421.
https://doi.org/10.1076/vesd.31.5.393.8361

[16] Wang X, Liu B, Gialleonardo ED, Kovacic I, Bruni S. Application of semi-active yow dampers for the improvement of the stability of high-speed rail vehicles: mathematical models and numerical simulation. Vehicle Syst Dyn. 2022;60(8):2608-2635.
https://doi.org/10.1080/00423114.2021.1912366

[17] Wilson N, Fires R, Witte M, Haigermoser A, Wrang M, Evans J et al. Assessment of safety against derailment using simulations and vehicle acceptance test: a worldwide comparison of state-of-the-art assessment methods. Vehicle Syst Dyn. 2011; 49(7):1113-1157.
https://doi.org/10.1080/00423114.2011.586706

[18] Zboiński K, Dusza M. Self-exciting vibrations and Hopf's bifurcation in non-linear stability analysis of rail vehicles in curved track. Eur J Mech A-Solid. 2010;29(2):190-203.
https://doi.org/10.1016/j.euromechsol.2009.10.001

[19] Zboiński K, Dusza M. Extended study of rail vehicle lateral stability in a curved track. Vehicle Syst Dyn. 2011;49(5):789-810.
https://doi.org/10.1080/00423111003770447

[20] Zboiński K, Dusza M. Bifurcation analysis of 4-axle rail vehicle models in a curved track. Nonlinear Dynam. 2017;89(2):863-885.
https://doi.org/10.1007/s11071-017-3489-y


## Appendix

### Parameters adopted to the modelled vehicle

Table A1. Mass parameters

| Variable | Description | Unit | Value |
|---|---|---|---|
| $m_{cb}$ | Car body mass | kg | 32 000 |
| $m_b$ | Bogie frame mass | kg | 2 600 |
| $m_w$ | Wheelset mass | kg | 1 800 |
| $m_{ab}$ | Axle box mass | kg | 100 |
| $m_r$ | Rail mass | kg | 60 |
| $m_s$ | Sleeper mass | kg | 500 |

Table A2. Vehicle model suspension parameters

| Variable | Description | Unit | Value | Comment |
|---|---|---|---|---|
| $k_{1x}$ | Longitudinal primary suspension stiffness | N/m | 30 000 000 | |
| $k_{1y}$ | Lateral primary suspension stiffness | N/m | 50 000 000 | |
| $k_{1z}$ | Vertical primary suspension stiffness | N/m | 732 000 | Preload force 46 500 N |
| $c_{1x}$ | Longitudinal primary suspension damping | N·s/m | 0 | |
| $c_{1y}$ | Lateral primary suspension damping | N·s/m | 0 | |
| $c_{1z}$ | Vertical primary suspension damping | N·s/m | 1 000<br>(Linear damping 7 000) | Nonlinear with series stiffness 600 kN/m |
| $k_{2x}$ | Longitudinal secondary suspension stiffness | N/m | 160 000 | |
| $k_{2y}$ | Lateral secondary suspension stiffness | N/m | 160 000 | |
| $k_{2z}$ | Vertical secondary suspension stiffness | N/m | 430 000 | Preload force 80 000 N |
| $c_{2x}$ | Longitudinal secondary suspension damping | N·s/m | 0 – nominal value<br>20 000 and 200 000 tested | Parameter tested in this article |
| $c_{2y}$ | Lateral secondary suspension damping | N·s/m | 8500<br>(Linear damping 1) | Nonlinear with series stiffness 6 000 kN/m |
| $c_{2z}$ | Vertical secondary suspension damping | N·s/m | 7100<br>(Linear damping 20 000) | Nonlinear with series stiffness 6 000 kN/m |
| $k_{bcb}$ | Bogie frame – car body secondary roll stiffness | N·m/rad | 16 406 | Torsion spring |

Table A3. Track model parameters

| Variable | Description | Unit | Value |
|---|---|---|---|
| $k_{vrs}$ | Rail – sleeper vertical stiffness | N/m | 50 000 000 |
| $k_{lrs}$ | Rail – sleeper lateral stiffness | N/m | 43 000 000 |
| $c_{vrs}$ | Rail – sleeper vertical damping | N·s/m | 200 000 |
| $c_{lrs}$ | Rail – sleeper lateral damping | N·s/m | 240 000 |
| $k_{rrs}$ | Rail – sleeper rolling stiffness | N/rad | 10 000 000 |
| $c_{rrs}$ | Rail – sleeper rolling damping | N·s/rad | 10 000 |
| $k_{vsg}$ | Sleeper – ground vertical stiffness | N/m | 1 000 000 000 |
| $k_{lsg}$ | Sleeper – ground lateral stiffness | N/m | 37 000 000 |
| $c_{vsg}$ | Sleeper – ground vertical damping | N·s/m | 1 000 000 |
| $c_{lsg}$ | Sleeper – ground lateral damping | N·s/m | 240 000 |
| $k_{rsg}$ | Sleeper – ground rolling stiffness | N·m/rad | 10 000 000 |
| $c_{rsg}$ | Sleeper – ground rolling damping | N·m·s/rad | 10 000 |

Table A4. Inertia parameters

| Variable | Description | Unit | Value |
|---|---|---|---|
| $i_{cbxx}$ | Car body inertia | kg·m$^2$ | 56 800 |
| $i_{cbyy}$ | | kg·m$^2$ | 1 970 000 |
| $i_{cbzz}$ | | kg·m$^2$ | 1 970 000 |
| $i_{bfxx}$ | Bogie frame inertia | kg·m$^2$ | 1 722 |
| $i_{bfyy}$ | | kg·m$^2$ | 1 476 |
| $i_{bfzz}$ | | kg·m$^2$ | 3 067 |
| $i_{wxx}$ | Wheelset inertia | kg·m$^2$ | 1 120 |
| $i_{wyy}$ | | kg·m$^2$ | 112 |
| $i_{wzz}$ | | kg·m$^2$ | 1 120 |
| $i_{axx}$ | Axlebox inertia | kg·m$^2$ | 20 |
| $i_{ayy}$ | | kg·m$^2$ | 12 |
| $i_{azz}$ | | kg·m$^2$ | 20 |

Table A5. Outside dimensions

| Variable | Description | | Unit | Value |
|---|---|---|---|---|
| $l_{cb}$ | Car body | length | m | 26.1 |
| $w_{cb}$ | | width | m | 2.83 |
| $h_{cb}$ | | height | m | 2.9 |
| $l_{bf}$ | Bogie frame | length | m | 3.06 |
| $w_{bf}$ | | width | m | 2.16 |
| $h_{bf}$ | | height | m | 0.84 |
| 2a | Wheelset | wheelbase | m | 2.5 |
| 2c | | axle length | m | 2.0 |
| 2b | | rolling circles distance | m | 1.5 |
| $r_t$ | | radius | m | 0.46 |